IEEE Photonics Journal
An IEEE Photonics Society Publication

Open Access

Experimental Investigations on Polarization Switching and Bistability in a 1550 nm VCSEL Subject to Orthogonal Optical Injection With Time-Varying Injection Power

Volume 12, Number 5, October 2020

Qian Wang
Guang-Qiong Xia
Zai-Fu Jiang
Wen-Yan Yang
Dian-Zuo Yue
Zheng-Mao Wu

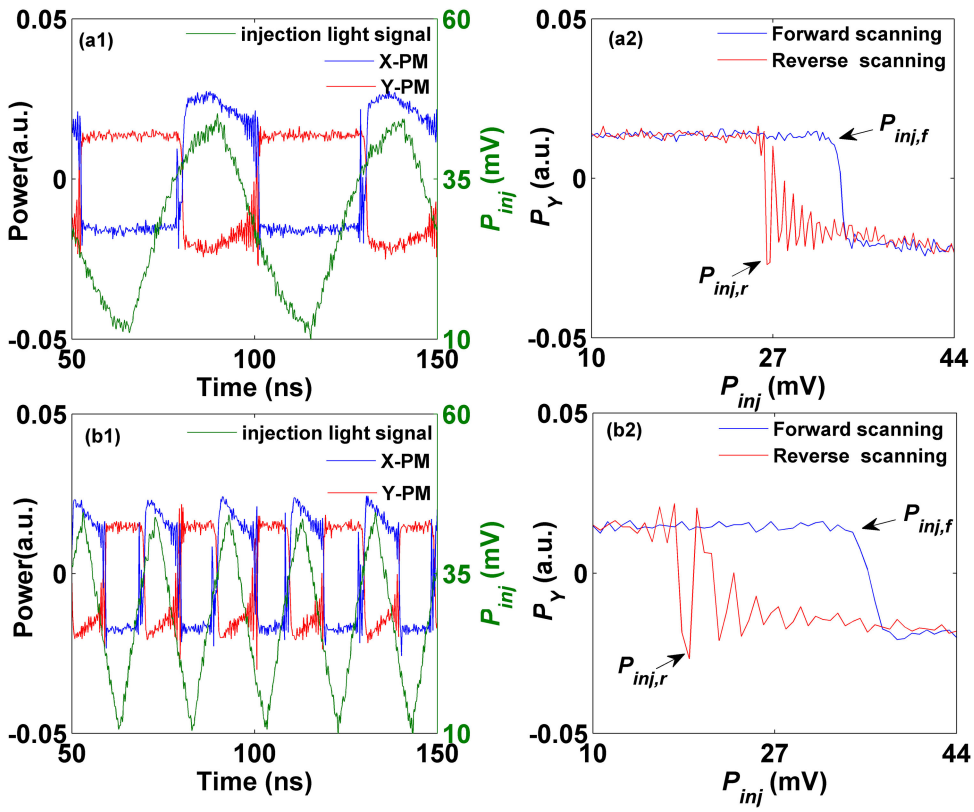

DOI: 10.1109/JPHOT.2020.3029054

Experimental Investigations on Polarization Switching and Bistability in a 1550 nm VCSEL Subject to Orthogonal Optical Injection With Time-Varying Injection Power

Qian Wang,[1] Guang-Qiong Xia,[1] Zai-Fu Jiang,[1] Wen-Yan Yang,[1,2] Dian-Zuo Yue,[1] and Zheng-Mao Wu[1]

[1]School of Physical Science and Technology, Southwest University, Chongqing 400715, China
[2]School of Mathematics and Physics, Chongqing University of Science and Technology, Chongqing 401331, China

DOI:10.1109/JPHOT.2020.3029054

Manuscript received September 17, 2020; revised September 30, 2020; accepted October 2, 2020. Date of publication October 7, 2020; date of current version October 16, 2020. This work was supported by the National Natural Science Foundation of China under Grants 61775184 and 61875167. Corresponding authors: Guang-Qiong Xia; Zheng-Mao Wu (e-mail: gqxia@swu.edu.cn; zmwu@swu.edu.cn).

Abstract: Polarization switching (PS) and polarization bistability (PB) characteristics of a 1550 nm vertical-cavity surface-emitting laser (VCSEL) subject to orthogonal optical injection (OOI) with time-varying injection power are experimentally investigated for the first time. To implement the optical injection, a Mach-Zehnder modulator (MZM) modulated by a triangular radio wave is adopted, and the influences of some typical parameters on the performances of PS and PB are analyzed. Under suitable operation conditions, PB in the VCSEL subject to OOI with time-varying injection power can be observed only for the input power P_0 of MZM locating within a determined range, and the width of hysteresis loop gradually decreases with the increase of P_0 from the minimum $P_{0,\min}$ to the maximum $P_{0,\max}$. Under different frequency detuning $\Delta\nu$ between the injection light and the X polarization mode of the VCSEL, the determined ranges of P_0 required for PB are different. With the variation of $\Delta\nu$ from a negative value to a positive value, both $P_{0,\min}$ and $P_{0,\max}$ present a trend of decrease first and then increase. Additionally, with the increase of the modulation frequency, the hysteresis loop width firstly increases rapidly and then gradually tends saturation.

Index Terms: Orthogonal optical injection (OOI), polarization bistability (PB), polarization switching (PS), time-varying injection power, vertical-cavity surface-emitting lasers (VCSELs).

1. Introduction

Vertical-cavity surface-emitting lasers (VCSELs) have received much attention due to their unique features, such as low threshold current, easy to integrate, high coupling efficiency with optical fibers, low manufacturing cost, *etc.* [1]. Due to weak material and cavity anisotropies, VCSELs can emit linearly polarization light along one of two orthogonal crystal directions. When the bias currents of the VCSELs are changed or additional degrees of freedom are introduced, polarization

switching (PS) between two polarization modes can occur [2]–[7]. If the PS points for forward scanning (gradually increasing the parameter value) and reverse scanning (gradually decreasing the parameter value) are different, polarization bistability (PB) may emerge. PS and PB in VCSELs have shown some promising applications, including all-optical logic gate, optical switching, optical storage, and so on [8]–[11].

A great deal of researches on PS and PB characteristics of VCSELs under free-running, optical feedback or optical injection have been reported. For free-running VCSELs, PS and PB induced by time-varying current have been investigated [12]–[15]. The results demonstrate that the sweep rate of the time-varying current affects the PS and PB characteristics of VCSELs, and rapidly scanning the current is helpful for increasing the width of the hysteresis loop [13], [14]. For VCSELs under optical feedback, through scanning the polarization direction and the feedback light strength, PS and PB can be observed, and the influences of the sweep rate have been analyzed [16]–[18]. Optical injection, as a commonly introduced perturbation for improving VCSELs performance such as reducing frequency chirp and enhancing modulation bandwidth [19]–[21], can also be employed to motivate PS and PB [22]–[31]. According to the polarized direction of the injection light relative to the dominant mode in a free-running VCSEL, optical injection can be categorized into orthogonal optical injection (OOI), parallel optical injection (POI) and variable polarization optical injection (VPOI). There are extensive investigations on the PB and PS performances of VCSELs under POI and VPOI [22]–[26]. For examples, Guo *et al.* experimentally observed frequency-induced ultra-wide hysteresis and power-induced hysteresis in VCSELs under POI [23]. Our group experimentally reported the influence of the polarization angle of optical injection on the PB characteristic in a VCSEL under VPOI [26]. Relevant researches on the PS and PB in VCSELs under OOI are also extensively reported [27]–[31]. Hurtado *et al.* experimentally observed three different shapes of power-induced hysteresis cycles in VCSELs under OOI, and analyzed the effect of bias current on PB [27], [28]. Also, the influences of the frequency detuning, injection power and bias current on PS and PB have been investigated [29]–[31].

We have noticed that the investigations on the PS and PB in VCSELs under OOI almost focus on the static case, *i. e.* scanning the injection parameter is implemented through manual operation. Under this circumstance, VCSELs have relaxed to their finial states before setting the injection parameter to the next value. Obviously, it is more practical and necessary to discuss the case of VCSELs subject to time-varying OOI by varying continuously the injection parameters in time. Few literatures have devoted to investigate theoretically the performances of PS and PB in VCSELs under time-varying OOI [32], [33]. Zhang *et al.* numerically studied the influences of the sweep rates of the time-varying injection intensity and time-varying frequency detuning on the PS and PB characteristics of VCSEL under OOI [32]. Salvide *et al.* numerically investigated the effects of bias current and injection intensity on the PB in VCSELs subject to OOI with time-varying frequency detuning [33]. However, to our knowledge, no relevant experimental results have been reported. As a result, in this work, we experimentally demonstrate the PS and PB in a 1550 nm VCSEL under time-varying OOI through scanning the injection power, and the influences of some typical parameters on the performances of PS and PB are analyzed.

2. Experimental Setup

Fig. 1 displays a schematic diagram of experimental setup. A commercial 1550 nm single-mode VCSEL is employed in this experiment. The bias current and temperature of the VCSEL are controlled by a high accuracy and low-noise current source (ILX-Lightwave, LDC-3724B) and the temperature is maintained at 21.3 °C during the whole experiment. A continuous light with power P_0 from a tunable laser (TL, Santec, TSL-710) is sent to a Mach-Zehnder modulator (MZM, iXblue, MXAN-LN-10, 10 GHz bandwidth), and then is modulated by a triangular radio wave from an arbitrary waveform generator (AWG, Tektronix, AWG70001A, 1.5 KSa/s - 50 GSa/s) and an electrical amplifier (EA, Agilent 83006). The output from the MZM is injected into the VCSEL after passing through a polarization controller 1 (PC1) and an optical circulator (OC) successively. PC1 is utilized to adjust the polarization of injection light to be orthogonal with the polarization direction of

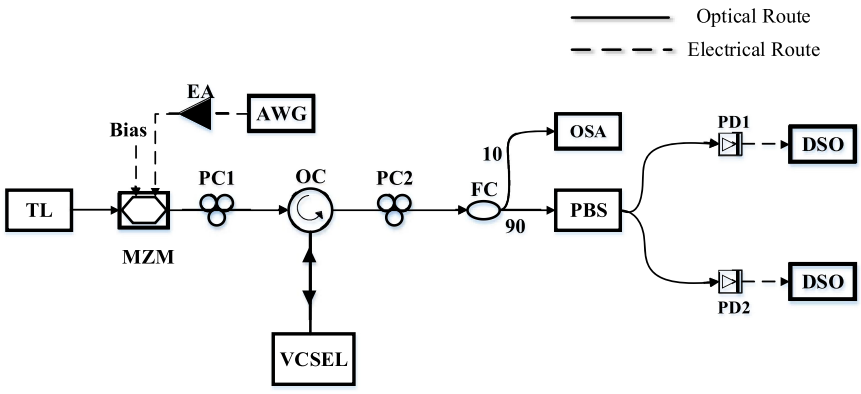

Fig. 1. Schematic of the experimental setup. TL: tunable laser; VCSEL: vertical-cavity surface-emitting laser; MZM: Mach-Zehnder modulator; AWG: arbitrary waveform generator; EA: electric amplifier; PM: power meter; PC: polarization controller; OC: optical circulator; FC: fiber coupler; PBS: polarization beam splitter; PD: photodiode; OSA: optical spectrum analyzer; DSO: digital storage oscilloscope.

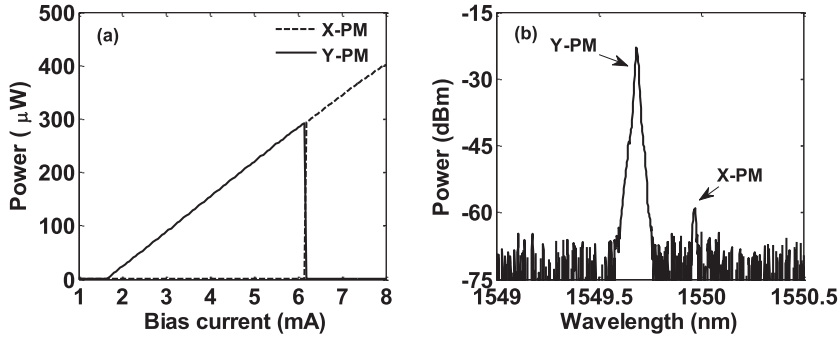

Fig. 2. (a) Polarization-resolved P-I curve of a solitary 1550 nm VCSEL. (b) Optical spectrum of the solitary VCSEL biased at $I = 3.5$ mA.

the dominant mode in the free-running VCSEL for realizing orthogonal optical injection (OOI). The output of the VCSEL successively passes through OC, PC2 and a 90:10 fiber coupler (FC), and then is sent to the detection system. The 10% branch of FC is sent to an optical spectrum analyzer (OSA, Ando AQ6317C) for measuring the optical spectrum, and the 90% branch of FC is sent to a polarization beam splitter (PBS) for separating X polarization mode (X-PM) and Y polarization mode (Y-PM), and their time series are recorded by a 20 GSa/s digital storage oscilloscope (DSO, Agilent 54855A) after transformed by two photodetectors (PD1, PD2, New Focus 1544B, 12 GHz bandwidth, 900 V/W conversion gain), respectively.

3. Results and Discussion

Fig. 2(a) shows the polarization-resolved P-I curve of the 1550 nm VCSEL at free-running, where the solid and the dashed lines represent Y-PM and X-PM, respectively. As seen in this diagram, Y-PM starts to lase at $I = 1.65$ mA. With the increase of I from 1.65 mA to 6.15 mA, the output power of Y-PM gradually increases while X-PM is always in a suppressed state. Once $I = 6.15$ mA, a sudden PS from Y-PM to X-PM occurs. After that, further increasing I to 8.00 mA, X-PM is always the dominant mode while Y-PM is always suppressed. In the following experiment, the bias current of the VCSEL is fixed at 3.5 mA. Under this case, the optical spectrum of the solitary VCSEL is shown in Fig. 2(b), where the dominant Y-PM and the suppressed X-PM are located at 1549.686 nm

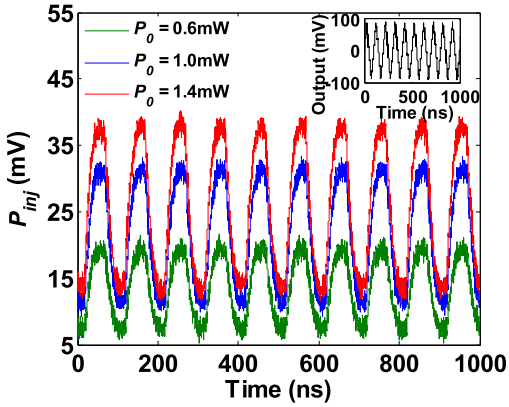

Fig. 3. Optical waveform output from the MZM under the modulation of a triangular radio wave with $f_m = 10$ MHz under different values of P_0, where the inset is the triangular radio wave.

and 1549.972 nm, respectively. Considering that the half-wave voltage of the utilized MZM in the experiment is about 5.5 V, the DC bias of MZM is set at 3 V to guarantee that the MZM operates within a linear region. During the experiment, the peak-to-peak value of the triangular radio wave generated by the AWG is fixed at 175.0 mV, and its frequency f_m can be adjusted. Under the modulation of a triangular radio wave, the MZM can output an optical triangular wave under suitable operating condition. Here, we label the input power of the MZM as P_0, and the output power of the MZM as P_{inj} after considering that the output of the MZM is taken as the injection light of the VCSEL. Fig. 3 records the waveform of the output light from the MZM modulated by a triangular radio wave under three different values of P_0, where the inset is the triangular radio wave with a frequency of $f_m = 10$ MHz. Obviously, under the modulation of a triangular radio wave, the optical wave output from the MZM is approximately triangular, and a larger P_0 results in a higher average power and peak-to-peak value of the output optical wave.

For orthogonal optical injection (OOI), the polarization direction of the injection light is required to be orthogonal with the polarization of the dominant mode of the free-running VCSEL. Since the dominant mode is Y-PM for the free-running VCSEL biased at 3.5 mA, the polarization direction of the injection light is adjusted to be along with X-PM for implementing OOI. For convenience, the frequency detuning $\Delta\nu$ is defined as $\Delta\nu = \nu_{inj} - \nu_X$, where ν_{inj} is the frequency of the injection light, and ν_X is the oscillation frequency of the X-PM of the VCSEL.

In the following, we will investigate PS and PB characteristics in the 1550 nm VCSEL under OOI with time-varying injection power. The waveforms for X-PM and Y-PM output from the 1550 nm VCSEL subject to OOI with $\Delta\nu = -3$ GHz and $f_m = 10$ MHz and the injection light signal are displayed in the left column of Fig. 4, where P_0 is 0.6 mW (Fig. 4(a1)) and 1.0 mW (Fig. 4(b1)), respectively. For $P_0 = 0.6$ mW, P_{inj} varies from 5.0 mV to 21.0 mV, and for $P_0 = 1.0$ mW, P_{inj} varies from 9.0 mV to 32.0 mV. Within multiple scanning periods, the dominant mode repeatedly switches between Y-PM and X-PM, and the corresponding hysteresis loop calculated in one cycle is presented in the right column of Fig. 4. Here, the hysteresis loop is obtained by recording the relationship of the output power of Y-PM (P_Y) and the injection power P_{inj}. It can be seen that P_Y behaves an oscillated variation for P_{inj} varies within certain parameter range, which is originated from the Y-PM operating at unstable state. After considering the oscillated characteristic of P_Y, the width of the hysteresis loop is determined by the interval between two specific P_{inj} represented by $P_{inj,f}$ and $P_{inj,r}$, where $P_{inj,f}$ ($P_{inj,r}$) is the injection power at which P_Y begins to decrease (increase) dramatically, and moreover no significant fluctuation for P_y can be observed for $P_{inj} > P_{inj,f}$ ($P_{inj} < P_{inj,r}$). The width of the hysteresis loop is 2.88 mV for $P_0 = 0.6$ mW and 1.75 mV for $P_0 = 1.0$ mW. Obviously, for different P_0, the width of hysteresis loop is different. The reason is that the variation rate of P_{inj} is different for different P_0.

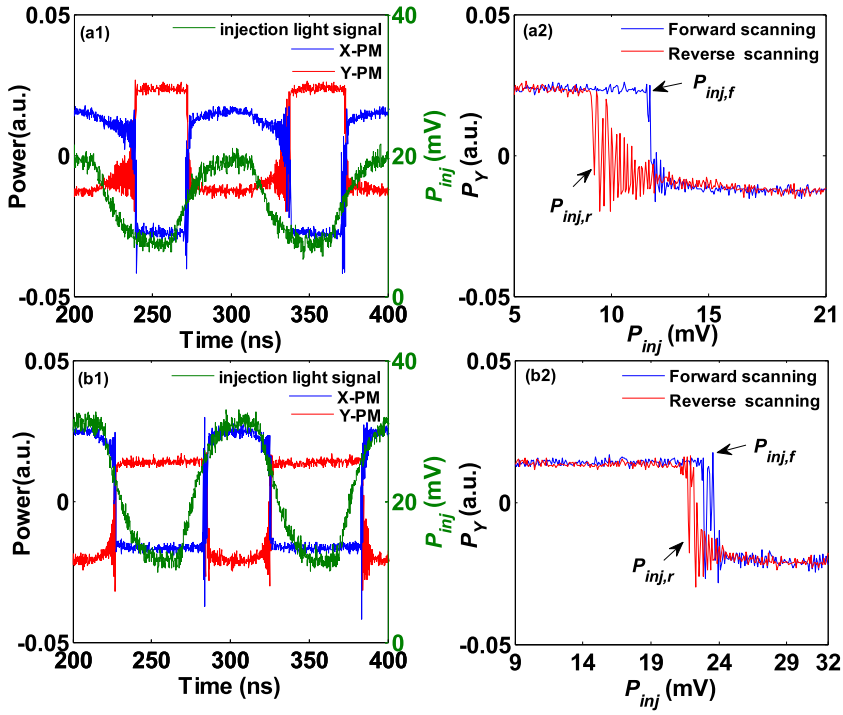

Fig. 4. Experimentally recorded waveforms (left column) and corresponding hysteresis loop (right column) for $\Delta\nu = -3$ GHz and $f_m = 10$ MHz under $P_0 = 0.6$ mW (a1-a2) and $P_0 = 1.0$ mW (b1-b2). The green lines are for the injection light signal.

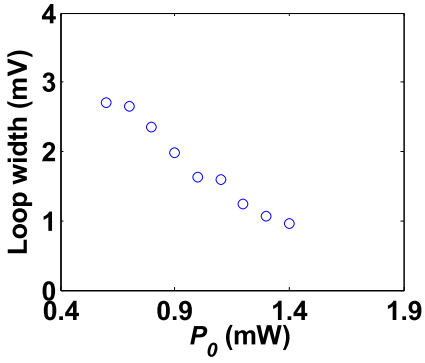

Fig. 5. Variation of the hysteresis loop width with P_0 under $\Delta\nu = -3$ GHz and $f_m = 10$ MHz.

The results shown in Fig. 4 show that the width of hysteresis loop is different for different P_0. Fig. 5 further describes the relationship of the hysteresis width with P_0 for the 1550 nm VCSEL subject to time-varying OOI with $\Delta\nu = -3$ GHz and $f_m = 10$ MHz. Here, the hysteresis loop width is obtained by averaging the widths calculated within 5 cycles after considering the influence of the noise. As shown in this diagram, PB can be observed within a range of P_0, where the minimum and maximum of P_0 required for achieving PB are labeled as $P_{0,\min}$ and $P_{0,\max}$, respectively. Under this experimental condition of $\Delta\nu = -3$ GHz and $f_m = 10$ MHz, $P_{0,\min}$ and $P_{0,\max}$ are 0.6 mW and 1.4 mW, respectively. With the increase of P_0 from $P_{0,\min}$ to $P_{0,\max}$, the hysteresis loop width gradually decreases.

Fig. 6 displays the experimentally measured $P_{0,\min}$ and $P_{0,\max}$ as a function of $\Delta\nu$ under $f_m = 10$ MHz. From this diagram, it can be seen that, with the increase of $\Delta\nu$ from -6 GHz to

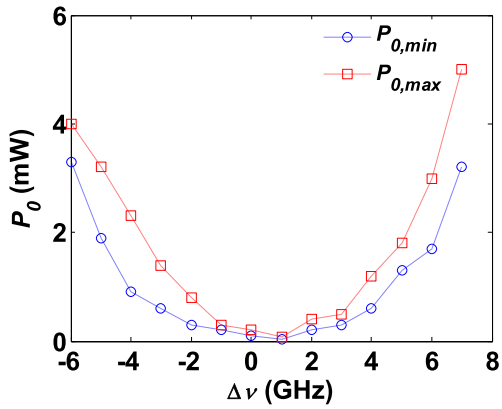

Fig. 6. Measured minimum and maximum P_0 required for PB as a function of $\Delta\nu$ under $f_m = 10$ MHz.

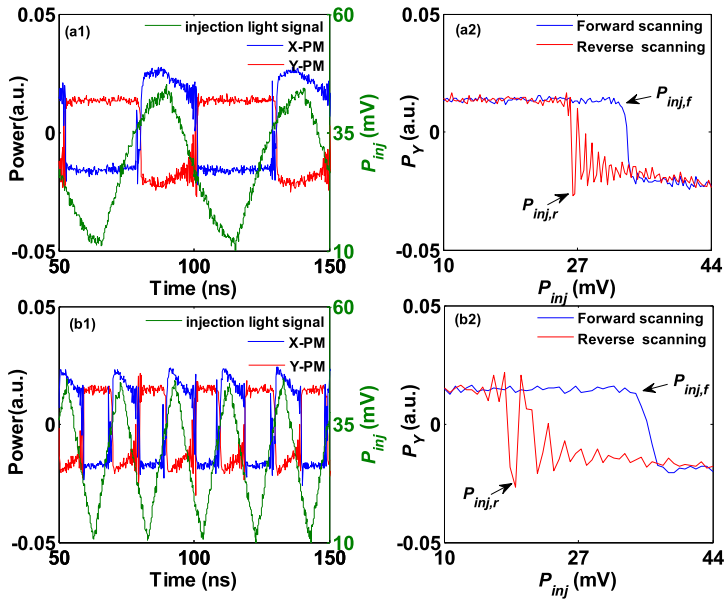

Fig. 7. Experimentally recorded waveform (left column) and corresponding hysteresis loop (right column) for $\Delta\nu$ = -4 GHz and $P_0 = 1.5$ mW under $f_m = 20$ MHz (a1-a2) and 50 MHz (b1-b2). The green lines are for the injection light signal.

7 GHz, both $P_{0,\min}$ and $P_{0,\max}$ first decrease, after reaching their minimum at $\Delta\nu = 1$ GHz, and then increase. Such a variation trend can be attributed to two factors: one is that the maximum and minimum of the time-varying injection power are depended on P_0, and the other is that the injection efficiency of OOI is related to $\Delta\nu$. As a result, through selecting different values of $\Delta\nu$, the region required for generating PB ($P_{0,\max}$ - $P_{0,\min}$) can be adjusted. Considering relatively large ($P_{0,max}$ - $P_{0,\min}$) can be obtained under $\Delta\nu$ = -4 GHz, in the following discussion, we set the value of $\Delta\nu$ at -4 GHz.

Above results are obtained under $f_m = 10$ MHz. Next, we will investigate the influence of the scanning frequency of the time-varying injection power. Fig. 7 shows the waveform (left column) output from the VCSEL subject to time-varying OOI with $\Delta\nu$ = -4 GHz and the injection light signal, and corresponding hysteresis loop (right column), where the injection light with a time-varying power is provided by the MZM injected by a continuous light with power of $P_0 = 1.5$ mW and modulated by a triangular radio wave with $f_m = 20$ MHz (upper row) and $f_m = 50$ MHz (below row), respectively. For $P_0 = 1.5$ mW, P_{inj} varies from 10.0 mV to 44.0 mV. For $f_m = 20$ MHz,

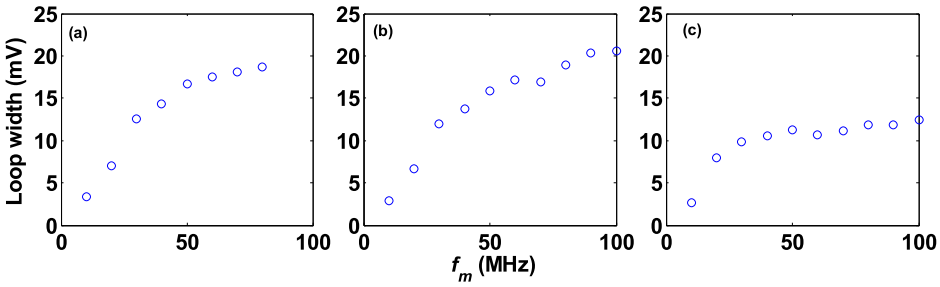

Fig. 8. Hysteresis loop width as a function of f_m for $\Delta\nu$ = -4 GHz under (a) P_0 = 1.1 mW, (b) 1.5 mW, and (c) 1.9 mW.

within multiple scanning periods, multiple PSs occur as shown in Fig. 7(a1). When P_{inj} decreases from 32.48 mV to 26.45 mV, the change of P_Y shows a fluctuation, and the width of the hysteresis loop is 6.31 mV (Fig. 7(a2)). For f_m = 50 MHz, more PS phenomena appear (Fig. 7(b1)), and the hysteresis width is broadened to be about 15.27 mV (Fig. 7(b2)). As a result, a larger f_m is helpful for achieving a wider hysteresis loop, which is consistent with the theoretical results reported in [Ref. 32].

Finally, the dependences of the hysteresis loop width on f_m are presented in Fig. 8 under $\Delta\nu$ = -4 GHz and different P_0. As shown in this diagram, for different values of P_0, the varied trends of the hysteresis loop width with f_m are approximately similar. With the increase of f_m, the hysteresis loop widths increase rapidly at the beginning, then increase lowly, and finally tend to saturation. In particular, for P_0 = 1.1 mW (Fig. 8(a)), no PB phenomenon occurs once f_m exceeds 80 MHz. However, for P_0 = 1.5 mW (Fig. 8(b)) and P_0 = 1.9 mW (Fig. 8(c)), PBs are always observed under $f_m \leq$ 100 MHz, and the saturated value of the hysteresis loop width under P_0 = 1.9 mW is smaller than that under P_0 = 1.5 mW.

4. Conclusion

In summary, we experimentally investigate the PS and PB characteristics in a 1550 nm VCSEL subject to time-varying orthogonal optical injection (OOI). The injection light with time-varying power is originated from a MZM subject to an optical injection with power P_0 and modulated by a triangular radio wave provided by an arbitrary waveform generator. During the experiment, the bias current of the 1550 nm VCSEL is fixed at 3.5 mA, and the peak-to-peak value of the triangular radio wave is fixed at 175.0 mV. The experimental results demonstrate that under suitable parameters, PB can be observed within a region of P_0, and the minimum and maximum within this region are labeled as $P_{0,\min}$ and $P_{0,\max}$, respectively. As P_0 increases from $P_{0,\min}$ to $P_{0,\max}$, the width of the hysteresis loop gradually decreases. With the increase of the frequency detuning $\Delta\nu$ between the injection light and the X-PM of the VCSEL from -6 GHz to 7 GHz, both $P_{0,\min}$ and $P_{0,\max}$ decrease firstly and then increase. For $\Delta\nu$ = 1 GHz, $P_{0,\min}$ and $P_{0,\max}$ reach their minimums. In addition, with the increase of f_m, the width of the hysteresis loop increases rapidly at the beginning, then increase slowly, and finally tend to saturation. We hope that this experimental work on the PS and PB operations of a 1550 nm VCSEL would be helpful for exploiting their practical applications in high-speed systems.

References

[1] F. Koyama, "Recent advances of VCSEL photonics," *J. Lightw. Technol.*, vol. 24, no. 12, pp. 4502–4513, Dec. 2006.
[2] Y. Hong, R. Jun, P. S. Spencer, and K. A. Shore, "Investigation of polarization bistability in vertical-cavity surface-emitting lasers subjected to optical feedback," *IEEE J. Quantum Electron.*, vol. 41, no. 5, pp. 619–624, May 2005.

[3] R. Vicente, J. Mulet, C. R. Mirasso, and M. Sciamanna, "Bistable polarization switching in mutually coupled vertical-cavity surface-emitting lasers," *Opt. Lett.*, vol. 31, no. 7, pp. 996–998, Apr. 2006.
[4] A. Quirce, A. Valle, L. Pesquera, H. Thienpont, and K. Panajotov, "Measurement of temperature-dependent polarization parameters in long-VCSELs," *IEEE J. Sel. Topics Quantum Electron.*, vol. 21, no. 6, pp. 636–642, Nov./Dec. 2015.
[5] M. F. Salvide, M. S. Torre, I. D. Henning, M. J. Adams, and A. Hurtado, "Dynamics of normal and reverse polarization switching in 1550-nm VCSELs under single and double optical injection," *IEEE J. Sel. Topics Quantum Electron.*, vol. 21, no. 6, pp. 643–651, Nov./Dec. 2015.
[6] V. N. Chizhevsky, "Dynamics of a bistable VCSEL subject to optical feedback from a vibrating rough surface," *IEEE J. Quantum Electron.*, vol. 54, no. 6, Dec. 2018, Art. no. 2400805.
[7] S. Nazhan and Z. Ghassemlooy, "Polarization output power stabilization of a vertical-cavity surface-emitting laser," *J. Opt. Soc. Am. B*, vol. 35, no. 7, pp. 1615–1619, Jul. 2018.
[8] J. Sakaguchi, T. Katayama, and H. Kawaguchi, "High switching-speed operation of optical memory based on polarization bistable vertical-cavity surface-emitting laser," *IEEE J. Quantum Electron.*, vol. 46, no. 11, pp. 1526–1534, Nov. 2010.
[9] S. Perrone, R. Vilaseca, and C. Masoller, "Stochastic logic gate that exploits noise and polarization bistability in an optically injected VCSEL," *Opt. Express*, vol. 20, no. 20, pp. 22692–22699, Sep. 2012.
[10] M. F. Salvide, C. Masoller, and M. S. Torre, "All-optical stochastic logic gate based on a VCSEL with tunable optical injection," *IEEE J. Quantum Electron.*, vol. 49, no. 10, pp. 886–893, Oct. 2013.
[11] T. Katayama, D. Hayashi, and H. Kawaguchi, "All-optical shift register using polarization bistable VCSEL array," *IEEE Photon. Technol. Lett.*, vol. 28, no. 19, pp. 2062–2065, Oct. 2016.
[12] C. Masoller, M. S. Torre, and P. Mandel, "Influence of the injection current sweep rate on the polarization switching of vertical-cavity surface-emitting lasers," *J. Appl. Phys.*, vol. 99, no. 2, Jan. 2006, Art. no. 026108.
[13] J. Paul, C. Masoller, Y. Hong, P. S. Spencer, and K. A. Shore, "Experimental study of polarization switching of vertical-cavity surface-emitting lasers as a dynamical bifurcation," *Opt. Lett.*, vol. 31, no. 6, pp. 748–750, Mar. 2006.
[14] J. Paul, C. Masoller, P. Mandel, Y. Hong, P. S. Spencer, and K. A. Shore, "Experimental and theoretical study of dynamical hysteresis and scaling laws in the polarization switching of vertical-cavity surface-emitting lasers," *Phys. Rev. A*, vol. 77, no. 4, Apr. 2008, Art. no. 043803.
[15] M. S. Torre and C. Masoller, "Dynamical hysteresis and thermal effects in vertical-cavity surface-emitting lasers," *IEEE J. Quantum Electron.*, vol. 46, no. 12, pp. 1788–1794, Dec. 2010.
[16] S. Y. Xiang *et al.*, "Variable-polarization optical feedback induced hysteresis of the polarization switching in vertical-cavity surface-emitting lasers," *J. Opt. Soc. Am. B*, vol. 27, no. 12, pp. 2512–2517, Dec. 2010.
[17] S. Nazhan, Z. Ghassemlooy, K. Busawon, and A. Gholami, "Investigation of polarization switching of VCSEL subject to intensity modulated and optical feedback," *Opt. Laser Technol.*, vol. 75, pp. 240–245, Dec. 2015.
[18] S. Nazhan and Z. Ghassemlooy, "Polarization switching dependence of VCSEL on variable polarization optical feedback," *IEEE J. Quantum Electron.*, vol. 53, no. 4, Aug. 2017, Art. no. 2400707.
[19] J. M. Liu, H. F. Chen, X. J. Meng, and T. B. Simpson, "Modulation bandwidth, noise, and stability of a semiconductor laser subject to strong injection locking," *IEEE Photon. Technol. Lett.*, vol. 9, no. 10, pp. 1325–1327, Oct. 1997.
[20] A. Gatto, A. Boletti, P. Boffi, and M. Martinelli, "Adjustable-chirp VCSEL-to-VCSEL injection locking for 10-Gb/s transmission at 1.55 microm," *Opt. Express*, vol. 17, no. 24, pp. 21748–21753, Nov. 2009.
[21] Y. Hong, P. S. Spencer, and K. A. Shore, "Wideband chaos with time-delay concealment in vertical-cavity surface-emitting lasers with optical feedback and injection," *IEEE J. Quantum Electron.*, vol. 50, no. 4, pp. 236–242, Apr. 2014.
[22] Y. Hong, P. S. Spencer, and K. Shore, "Power and frequency dependence of hysteresis in optically bistable injection-locked VCSELs," *Electron. Lett.*, vol. 37, no. 9, pp. 569–570, Apr. 2001.
[23] P. Guo, W. J. Yang, D. Parekh, C. J. Chang-Hasnain, A. S. Xu, and Z. Y. Chen, "Experimental and theoretical study of wide hysteresis cycles in 1550 nm VCSELs under optical injection," *Opt. Express*, vol. 21, no. 3, pp. 3125–3132, Feb. 2013.
[24] A. Quirce *et al.*, "Polarization switching and injection locking in vertical-cavity surface-emitting lasers subject to parallel optical injection," *Opt. Lett.*, vol. 41, no. 11, pp. 2664–2667, Jun. 2016.
[25] F. Denis-le Coarer *et al.*, "Polarization dynamics induced by parallel optical injection in a single-mode VCSEL," *Opt. Lett.*, vol. 42, no. 11, pp. 2130–2133, Jun. 2017.
[26] J. J. Chen *et al.*, "Polarization bistability in a 1550 nm vertical-cavity surface-emitting laser subject to variable polarization optical injection," *IEEE Photon. J.*, vol. 9, no. 2, Apr. 2017, Art. no. 1502309.
[27] A. Hurtado, I. D. Henning, and M. J. Adams, "Two-wavelength switching with a 1550 nm VCSEL under single orthogonal optical injection," *IEEE J. Sel. Topics Quantum Electron.*, vol. 14, no. 3, pp. 911–917, May/Jun. 2008.
[28] A. Hurtado, A. Quirce, A. Valle, L. Pesquera, and M. J. Adams, "Power and wavelength polarization bistability with very wide hysteresis cycles in a 1550nm-VCSEL subject to orthogonal optical injection," *Opt. Express*, vol. 17, no. 26, pp. 23637–23642, Dec. 2009.
[29] M. Torre, A. Hurtado, A. Quirce, A. Valle, L. Pesquera, and M. Adams, "Polarization switching in long-wavelength VCSELs subject to orthogonal optical injection," *IEEE J. Quantum Electron.*, vol. 47, no. 1, pp. 92–99, Jan. 2011.
[30] A. Qader, Y. Hong, and K. A. Shore, "Role of suppressed mode in the polarization switching characteristics of optically injected VCSELs," *IEEE J. Quantum Electron.*, vol. 49, no. 2, pp. 205–210, Feb. 2013.
[31] A. A. Qader, Y. Hong, and K. A. Shore, "Ultra-wide hysteresis frequency bistability in vertical cavity surface emitting lasers subject to orthogonal optical injection," *Appl. Phys. Lett.*, vol. 103, no. 2, Jul. 2013, Art. no. 21108.
[32] W. L. Zhang, W. Pan, B. Luo, M. Y. Wang, and X. H. Zou, "Polarization switching and hysteresis of VCSELs with time-varying optical injection," *IEEE J. Sel. Topics Quantum Electron.*, vol. 14, no. 3, pp. 889–894, May/Jun. 2008.
[33] M. F. Salvide, C. Masoller, and M. S. Torre, "Polarization switching and hysteresis in vertical-cavity surface-emitting lasers subject to orthogonal optical injection," *IEEE J. Quantum Electron.*, vol. 50, no. 10, pp. 848–853, Oct. 2014.